Cobalt-modified molybdenum carbide as a selective catalyst for hydrodeoxygenation of furfural

Zhexi Lin[a], Weiming Wan[a], Siyu Yao[b], Jingguang G. Chen[a,b,*]

[a] Department of Chemical Engineering, Columbia University, New York, NY, 10027, United States
[b] Chemistry Division, Brookhaven National Laboratory, Upton, NY, 11973, United States

ABSTRACT

The hydrodeoxygenation (HDO) reaction is crucial to the upgrading of biomass-derived furfural to produce a promising fuel additive, 2-methylfuran. In order to enhance the stability of the molybdenum carbide (Mo_2C) catalyst, this work utilizes cobalt (Co) modification to tune the oxygen and furfural binding energies on Mo_2C. Density functional theory (DFT) calculations of the adsorption configuration of furfural on $Mo_2C(0001)$ and cobalt-modified molybdenum carbide ($Co/Mo_2C(0001)$) reveal that the C=O bond of furfural is elongated, facilitating the selective C=O scission to produce 2-methylfuran. The reduced oxygen and furfural binding energies on $Co/Mo_2C(0001)$ allow the facile removal of surface oxygen and furfural to improve the stability of the catalyst. Temperature-programmed desorption (TPD) experiments on model surfaces confirm the enhanced stability and overall HDO performance of $Co/Mo_2C/Mo(110)$. Based on the results from high-resolution electron energy loss spectroscopy (HREELS), 2-methylfuran-like intermediates are observed on both $Mo_2C/Mo(110)$ and $Co/Mo_2C/Mo(110)$. Parallel reactor evaluations over the corresponding powder catalysts further demonstrate the enhanced stability of Co/Mo_2C over Mo_2C at ambient pressure. This work illustrates the important roles of oxygen and furfural binding energies in the furfural HDO reaction on both model surfaces and powder catalysts, which in turn provides insights into designing selective and stable carbide-based catalysts for HDO reactions.

1. Introduction

The catalytic upgrading of biomass into chemicals and fuels is a promising method to address the current energy and environmental challenges [1–5]. Many biomass-derived molecules contain excess oxygen, which leads to low energy density and undesired reactivity to produce byproducts [6] when used directly in the fuel and chemical sectors. In order to convert these molecules into more valuable products, the excess oxygen needs to be selectively removed via the hydrodeoxygenation (HDO) reaction without carbon-carbon bond scission. Among the biomass derivatives, furfural is a promising platform chemical that can be produced from the dehydration of xylose, a derivative from hemicellulose [7]. Furfural is an example of the over-functionalized molecules that can be upgraded efficiently with the HDO reaction.

In this work, we focused on the conversion of furfural into 2-methylfuran (2-MF), which is a promising fuel additive due to its high blending research octane number [7]. In the conversion from furfural to 2-MF, C=O bond cleavage of the external carbonyl group is required via the HDO reaction. To selectively break the C=O bond, a catalyst should bind to oxygen strongly enough to cleave the C=O bond to produce 2-MF and atomic oxygen, but weakly enough so that the oxygen atom can be easily removed to complete the catalytic cycle. Thus, the oxygen binding energy of the catalyst should play an important role in controlling the catalytic activity and stability. Previously, copper-based catalysts have been reported to be active for the furfural HDO reaction [8]. However, these reactions used copper chromite, which is toxic and non-environmental friendly. More recently, bimetallic catalysts $FeNi/SiO_2$ and bimetallic surfaces Fe/Ni (111) and Co/Pt(111) were reported to selectively convert furfural to 2-MF [9–11]. Bimetallic catalysts typically possess different d-band characteristics and thus different binding energies from their parent metals. This unique property allows the tuning of the activity and selectivity of the monometallic catalysts with admetals [12]. However, this unique property is structurally dependent. For example, it was reported that the structure of a Co-overlayer deposited on Pt(111) showed higher 2-MF activity than the Pt/Co/Pt(111) subsurface structure [11]. At elevated temperatures, the Co-overlayer on Pt can easily diffuse into the subsurface, decreasing the HDO activity for 2-MF production.

On the other hand, molybdenum carbide (Mo_2C) possesses similar bulk electronic properties to Pt [13] and can also serve as a diffusion barrier to prevent the metal overlayer from diffusing into the subsurface [14], making it a good substrate to maintain the metal overlayer structure. By replacing the Pt substrate with Mo_2C, the cost of the catalyst can also be significantly reduced. In addition, Mo_2C is a selective catalyst for the C=O bond scission. For example, Mo_2C has been shown as a highly selective catalyst for the HDO reaction of C3 molecules, such as propanol and propanal, to produce propylene [15]. Mo_2C was also reported to selectively convert furfural to 2-MF but deactivated quickly [16]. The cause of the deactivation was considered to be poisoned by the strong bonding of atomic oxygen [17] and the polymeric derivatives of furfural [16] by blocking the active sites on Mo_2C.

It has been reported that admetals can be used to modify the binding energies of carbon, oxygen and hydrogen on Mo_2C [18]. This property can potentially be used to reduce the furfural and oxygen binding energies on Mo_2C to enhance the stability of the catalyst. In order to solve the stability issues associated with the bimetallic and Mo_2C catalysts, this work combines the advantages of both types of catalysts and uses Co overlayer to modify Mo_2C. In this way, the Co overlayer reduces the oxygen and furfural binding energies on Mo_2C to prevent the poison by these adsorbates to increase the catalyst stability, and the Mo_2C substrate serves as a diffusion barrier to stabilize the Co overlayer structure. Density functional theory (DFT) was used to calculate the binding energies and bond lengths of furfural on $Mo_2C(0001)$ and $Co/Mo_2C(0001)$. The gas-phase products were determined using temperature-programmed desorption (TPD) and the surface intermediates and adsorption configurations were identified using high-resolution electron energy loss spectroscopy (HREELS) under ultra-high vacuum (UHV) conditions. Parallel flow reactor experiments were performed to verify the stability trend between Mo_2C and Co/Mo_2C powder catalysts at ambient pressure.

2. Experimental and theoretical methods

2.1. DFT calculations

All DFT calculations were preformed using the Vienna *Ab initio* Simulation Package (VASP) [19–21] with the Projector Augmented Wave (PAW) method [22]. Generalized Gradient Approximation (GGA) [23] and the PW91 functional [24] were used with a kinetic cutoff energy of 400 eV. The total energies were minimized self-consistently using a convergence threshold of 10^{-6} eV. The nuclear degrees of freedom were optimized to a force convergence threshold of 0.05 eV Å^{-1}. A periodic 4×4 unit cell and a $3 \times 3 \times 1$ Monkhorst–Pack k-point grid were used for all slabs. The lattice constants of Mo-terminated Mo_2C (0001) was previously reported [25]. The $Mo_2C(0001)$ surface was modeled by adding 20 Å of vacuum onto a slab containing six alternate layers of Mo and C, with a ratio of Mo/C = 2. The Co-modified $Mo_2C(0001)$ surface was modeled by adding an atomic layer of Co over the Mo_2C surface. The metal overlayer and the top Mo_2C layer were allowed to relax. The calculations were carried out with the implementation of spin-polarization. The binding energy of the adsorbate on each surface was calculated by subtracting the free energies of the slab and gas-phase adsorbate from that of the slab with adsorbate.

2.2. Surface science experiments

The TPD experiments were carried out in an ultra-high vacuum (UHV) chamber with a base pressure of 5×10^{-10} Torr. The chamber is equipped with an Auger electron spectrometer (AES), a mass spectrometer (MS), a sputter gun and metal sources as previously described [26]. A Mo(110) single crystal was spot-welded to two tantalum posts for resistive heating. A K-type thermocouple was spot-welded to the back of the crystal for temperature measurements. The HREELS

experiments were performed in a separate UHV chamber equipped with similar instruments as the TPD chamber in addition to the HREELS spectrometer, as reported previously [27]. Samples were prepared in the upper chamber and subsequently lowered to the HREELS chamber for measurements.

The procedure for preparing carbide-modified Mo(110) has been previously reported [28]. In a typical experiment, the Mo(110) crystal was cleaned using Ne$^+$ sputtering at 1000 K, followed by annealing to 1200 K. Trace amount of carbon on the surface was titrated with oxygen at 1000 K and subsequently annealed to 1200 K. Carbide-modified Mo(110) surface, as a model surface for Mo_2C, was synthesized using cycles of ethylene dosing at 600 K and annealing to 1200 K until a Mo/C atomic ratio of 2:1 was reached. Based on previous literature, the as-synthesized surface should be Mo-terminated with a p(4 × 4) LEED pattern [29,30]. The Co overlayer was deposited onto the $Mo_2C/Mo(110)$ surface using a metal evaporation source. 5 L of hydrogen, corresponding to half of the saturation coverage of atomic hydrogen, followed by 4 L of furfural were introduced into the chamber through a stainless steel dosing line. For TPD experiments, the surfaces were ramped at 3 K/s and the desorbed gases were detected by the MS. For HREELS experiments, the samples were flashed to the desired temperatures at 3 K/s and then cooled down to 100 K before the spectra were recorded.

Furfural (Sigma–Aldrich, 99%) was transferred into a stainless steel cylinder under N_2 atmosphere and subsequently purified using freeze-pump-thaw cycles. Ethylene, hydrogen, oxygen, neon and carbon monoxide gases were of research purity and were used without further purification.

2.3. Synthesis and characterization of powder Mo_2C and Co/Mo_2C catalysts

Ammonium molybdate tetrahydrate (99.98%, Sigma) was grinded and calcined in a muffle oven with a ramp rate of 10 K/min to 773 K to synthesize MoO_3. To carburize MoO_3, 40 mg of the as-synthesized MoO_3 was heated in a quartz tube reactor using a mixture of H_2 and CH_4 (45 mL/min; 90/10 v/v) at a ramp rate of 5 K/min to 573 K and held for 2 h. The sample was then ramped to 973 K at 0.5 K/min and held at 973 K for 2 h. Then the sample was cooled to 750 K and held for 1 h and the gas was switched to 40 mL/min H_2 to reduce the carburized β-Mo_2C sample.

Co/MoO_3 was synthesized first by dropwise adding an appropriate amount of cobalt (II) nitrate hexahydrate solution to the ammonium molybdate tetrahydrate solution under stirring. The precipitate formed was dried at 393 K for 3 h and calcined in a muffle oven to 773 K at a ramp rate of 10 K/min. 40 mg of the as-synthesized Co/MoO_3 was carburized and reduced using the same procedure as that for MoO_3.

XRD patterns of the powder catalysts were obtained using a Rigaku Ultima X-Ray Diffractometer equipped with a Ni filtered Cu Kα radiation source operated at 40 kV and 44 mA. Each sample was scanned at a step size of 0.01° at a rate of 6°/min between 20° and 80°.

2.4. Reactor experiments

The vapor phase reaction of furfural over powder catalysts was carried out at atmospheric pressure in a quartz tube reactor housed within a tube furnace (Applied Test System). All flow lines were heated to above 453 K to prevent the condensation of effluent. After the reduction of the Mo_2C and Co/Mo_2C catalysts at 750 K, the temperature was lowered to the reaction temperature of 523 K, at which point the gases were switched to 20 mL/min H_2. After obtaining a stable baseline, furfural vapor at a space velocity of 0.10 mL/(g_{cat}*s) was introduced into the quartz tube reactor by directing the H_2 through a bubbler containing furfural preheated to 323 K. The molar ratio of hydrogen to furfural was 80. The gas effluent from the reactor was measured by a residual gas analyzer (Stanford Research System RGA200) equipped with a quadruple mass spectrometer.
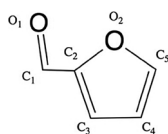
Scheme 1. Atomic assignment of the furfural molecule.

3. Results and discussion

3.1. DFT calculations

DFT calculations were performed to investigate the adsorption configurations of furfural on $Mo_2C(0001)$ and $Co/Mo_2C(0001)$. The atomic assignment is shown in Scheme 1 and the side views of adsorbed furfural are shown in Fig. 1. Table 1 summaries the C1−C2 and C1−O1 bond lengths and the binding energies of furfural on the two surfaces. Compared to gas phase furfural, the C1−O1 bonds of adsorbed furfural on the $Co/Mo_2C(0001)$ and $Mo_2C(0001)$ surfaces are both elongated, consistent with a $\eta^2(C,O)$ bonding configuration via the carbonyl group. The elongated C1-O1 bonds should facilitate the C1−O1 bond scission and the subsequent 2-MF formation on both surfaces. In addition, the C1−C2 bonds are shortened on both surfaces, indicating that the C−C bond scission pathway to form furan is not preferred.

As summarized in Table 1, the oxygen and furfural binding energies are both stronger on $Mo_2C(0001)$ than on $Co/Mo_2C(0001)$. This difference suggests that the surface oxygen and furfural can be more easily removed from $Co/Mo_2C(0001)$ during the reaction, leaving the active sites open for the subsequent reaction. Under UHV conditions, surface oxygen is likely to recombine with surface carbon and desorb in the form of CO; under reactor condition at ambient pressure with excess hydrogen, surface oxygen can be removed in the form of water. Since furfural likely undergoes polymerization [16], a lower furfural binding energy should facilitate the desorption of furfural to avoid the poisoning by furfural and related polymeric species.

In addition, since it is not likely for the Co coverage of the powder catalysts to be exactly one monolayer (1ML), the Co-Mo interface and multilayer Co on Mo_2C surfaces were briefly investigated. Calculations on the Co-Mo interface suggests that furfural adsorbs in an unstable geometry and the furfural binding energy on the Co site is much lower than that on the Mo sites, which could potentially result in a lower 2-MF activity on this interface. On the other hand, the similar furfural binding energies on surfaces with Co coverage beyond 1 ML should suggest similar 2-MF activities on these surfaces (Table S1 in Supplementary material).

3.2. TPD results on model surfaces

TPD experiments were performed on $Mo_2C/Mo(110)$ and $Co/Mo_2C/Mo(110)$ surfaces to determine the gas-phase products from the reactions and the stability of the surfaces. Fig. 2 (a) and (b) show the TPD spectra of 2-MF desorbed from $Mo_2C/Mo(110)$ and monolayer (1 ML) $Co/Mo_2C/Mo(110)$ in three successive experiments without cleaning

Table 1

Comparison of the bond lengths (Å) and binding energies (eV) of furfural on $Mo_2C(0001)$, $Co/Mo_2C(0001)$.

	C_1-O_1(Å)	C_1-C_2(Å)	$\dfrac{d(C_1-O_1)}{d(C_1-C_2)}$	Furfural binding energy (eV)	Oxygen binding energy (eV)
Gas phase	1.232	1.452	0.848		
$Mo_2C(0001)$	1.36	1.422	0.956	− 3.62	− 9.467
$Co/Mo_2C(0001)$	1.349	1.416	0.953	− 2.087	− 7.963

the surface after each TPD measurement. As shown in Fig. 2 (a), for the first TPD experiment, a relatively large amount of 2-MF desorbs from Mo_2C at 263 K. However, for the second and third TPD experiments, the yield of 2-MF decreases significantly. In contrast, Fig. 2 (b) shows that a nearly constant amount of 2-MF desorbs at 301 K from $Co/Mo_2C/Mo(110)$ in the three successive TPD experiments.

Comparing the results from the first TPD experiments, the 2-MF yield of $Mo_2C/Mo(110)$ is higher than that of $Co/Mo_2C/Mo(110)$, which is consistent with the trend of oxygen binding energies shown in Table 1. The high oxygen binding energy of $Mo_2C/Mo(110)$ promotes the C=O bond cleavage and improves the HDO activity, but also obstructs the removal of the surface oxygen. Comparing the stability for 2-MF production between the two surfaces, $Mo_2C/Mo(110)$ deactivates rapidly after the first TPD experiment, while $Co/Mo_2C/Mo(110)$ maintains comparable activity in subsequent TPD experiments. Fig. 2(c) shows the CO desorption in the first TPD experiments of both surfaces. No CO desorbs from $Mo_2C/Mo(110)$, while there are two CO desorption peaks from $Co/Mo_2C/Mo(110)$ resulting from the removal of surface oxygen by reacting with carbon. These results suggest that $Mo_2C/Mo(110)$ binds to oxygen too strongly such that the atomic oxygen remain on the surface, blocking the active sites and poisoning the catalytic surface. But the lower oxygen binding energy of $Co/Mo_2C/Mo(110)$ facilitates the facile removal of surface oxygen during the reaction, leaving the active sites available for the next reaction.

Quantification of the gas-phase products is achieved using a previously reported procedure [31]. The results (Table 2) indicate that 2-MF and furan are the two furanic compounds observed. The reaction pathways for 2-MF and furan formation are shown in Scheme 2. The selectivity to 2-MF is 85 % for $Mo_2C/Mo(110)$ and 72 % for $Co/Mo_2C/Mo(110)$. Similar to the 2-MF production, the furan production on $Mo_2C/Mo(110)$ decreases rapidly after the first TPD experiment. This again suggests that the surface deactivated after the first TPD experiment. Meanwhile, on $Co/Mo_2C/Mo(110)$ the activities for 2-MF and furan production remain relatively constant for the three successive TPD experiments, indicating that the stability of $Co/Mo_2C/Mo(110)$ is better than that of $Mo_2C/Mo(110)$.

Investigation of the effect of cobalt coverage on the 2-MF activity suggests that the Mo-Co interface is slightly less active towards 2-MF production compared to the $Mo_2C/Mo(110)$ and 1 ML $Co/Mo_2C/Mo(110)$ surfaces, while surfaces with Co coverage greater than 1 ML show similar 2-MF activities, consistent with the DFT calculations (Fig. S1
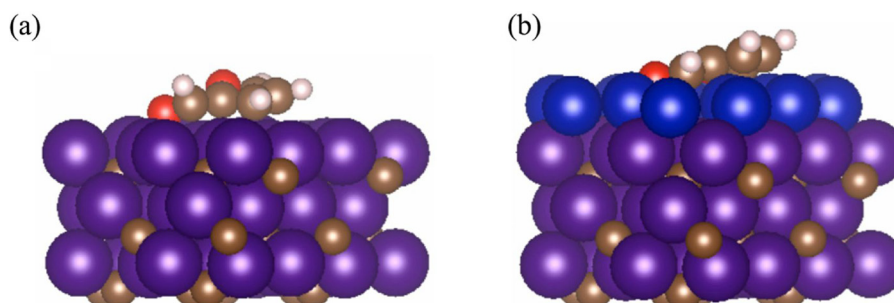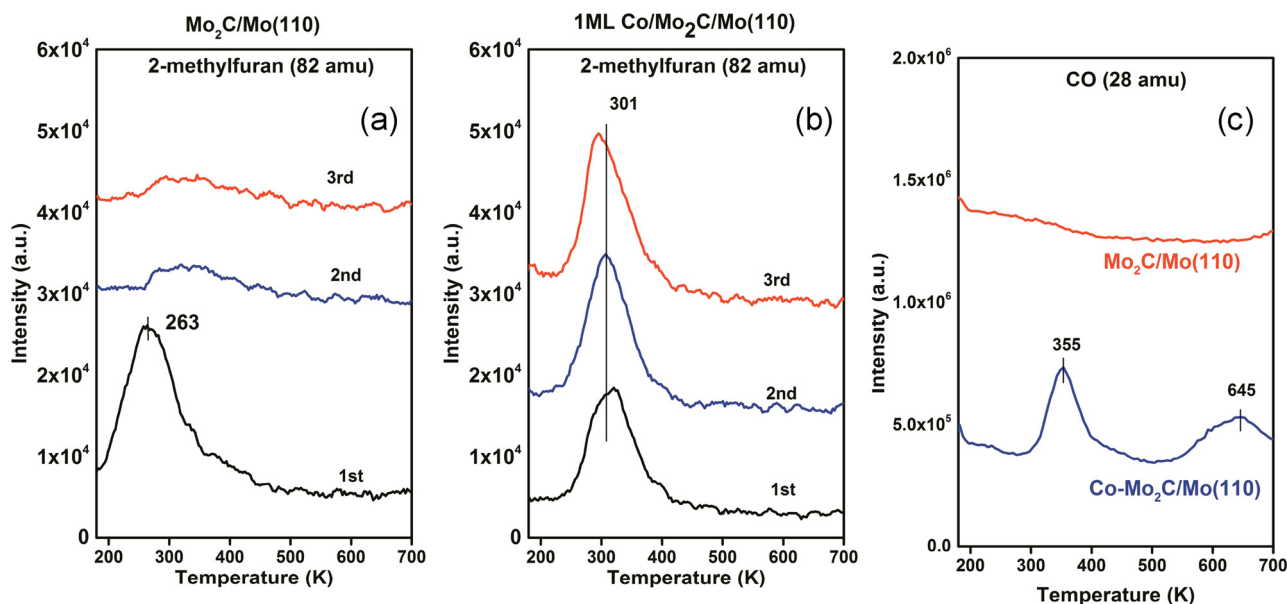
(a)

(b)

Fig. 1. Side views of furfural absorbed on (a) $Mo_2C(0001)$ and (b) $Co/Mo_2C(0001)$.

Fig. 2. (a) and (b): Spectra of 2-MF (82 amu) with an exposure of 4 L furfural on hydrogen pre-dosed (a) $Mo_2C/Mo(110)$ and (b) monolayer (1 ML) $Co/Mo_2C/Mo$ (110) surfaces from three successive experiments; (c): Spectra of CO (28 amu) with an exposure of 4 L furfural on corresponding hydrogen pre-dosed surfaces.

Table 2
Activities (molecules per metal atom) for the production of furanic compounds on hydrogen pre-dosed surfaces from TPD experiments.

	2-MF	Furan	Total activity of furanic compound
$Mo_2C/Mo(110)$ 1st	0.0249	0.0043	0.0292
$Mo_2C/Mo(110)$ 2nd	0.0041	0.0000	0.0041
$Mo_2C/Mo(110)$ 3rd	0.0037	0.0000	0.0037
1 ML $Co/Mo_2C/Mo(110)$ 1st	0.0144	0.0040	0.0185
1 ML $Co/Mo_2C/Mo(110)$ 2nd	0.0149	0.0041	0.0189
1 ML $Co/Mo_2C/Mo(110)$ 3rd	0.0152	0.0058	0.0210

Table 3
Vibrational mode assignment for furfural molecule.

Mode	Frequency (cm^{-1})		
	Raman[32]	H/Ni(111)[10]	H/$Mo_2C/Mo(110)$[a]
ω_{ring}(C-H)		771	765
ν_{ring}(C-O)	1025		1060
ν_{ring}(C=C)	1446	1448	1436
$\nu_{aliphatic}$(C=O)	1684	1637	1624
$\nu_{aliphatic}$(C-H)		2882	2852
ν_{ring}(C-H)	3153	3112	3067

Abbreviation: ω – wagging, ν – stretching.
[a] 4 L furfural on hydrogen predosed $Mo_2C/Mo(110)$ at 100 K.
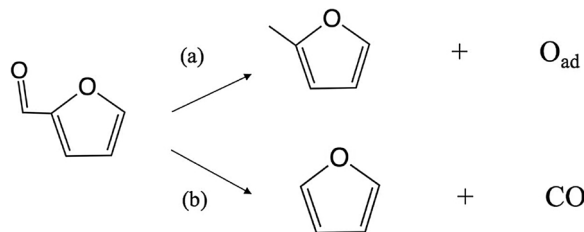
Scheme 2. Possible reaction pathways of furfural on $Mo_2C/Mo(110)$ and Co/$Mo_2C/Mo(110)$: (a) 2-MF formation; (b) furan formation.

and Table S1 in Supplementary material). The results on the stabilities of $Mo_2C/Mo(110)$, 0.25 ML, 1 ML and 2 ML $Co/Mo_2C/Mo(110)$ show that the presence of Co enhances the stability of not only 1 ML Co/Mo_2C, but also partially covered or multilayer Co/Mo_2C surfaces (Fig. S2).

3.3. HREELS measurements

HREELS experiments were performed to identify the adsorption configurations of furfural and reaction intermediates on the Mo_2C/Mo (110) and $Co/Mo_2C/Mo(110)$ surfaces. The assignments for the vibrational modes of furfural molecule are shown in Table 3. Fig. 3 (a) compares the spectra of furfural on $Mo_2C/Mo(110)$ at different temperatures. The spectrum of molecularly absorbed furfural at 100 K generally matches the Raman spectrum of liquid-phase furfural [32]. The vibrational peaks at 1060 cm^{-1} (ν_{ring}(C–O)), 1436 cm^{-1} (ν_{ring}(C=C)), 1624 cm^{-1} ($\nu_{aliphatic}$(C=O)) and 3067 cm^{-1} (ν_{ring}(C–H))

are characteristic of furfural. After increasing the temperature to 200 and 250 K, the relative intensity of the peak at 1624 cm^{-1} ($\nu_{aliphatic}$(C=O)) decreases, suggesting that the C=O bond in the carbonyl group is weakened. This is consistent with the DFT calculation that furfural binds to the surface in a η^2(C,O) bonding configuration via the carbonyl group. The intensity of the peak at 2854 cm^{-1} ($\nu_{aliphatic}$(C–H)) increases as the temperature increases, likely due to the hydrogenation of the carbonyl group. This is consistent with previous literature [33] that the hydrogenation of the carbonyl group is a critical step to the formation of 2-MF.

Fig. 3 (b) compares the HREEL spectra of molecularly adsorbed 2-MF on Mo_2C and the surface intermediates at 200 K on $Mo_2C/Mo(110)$ and $Co/Mo_2C/Mo(110)$ after dosing furfural and hydrogen on the surfaces. The spectra of furfural on $Mo_2C/Mo(110)$ and $Co/Mo_2C/Mo(110)$ show the characteristic vibrational modes of molecularly adsorbed 2-MF, indicating the formation of intermediates similar to 2-MF on both surfaces. This is consistent with the 2-MF onset desorption temperatures of 200 K ($Mo_2C/Mo(110)$) and 235 K ($Co/Mo_2C/Mo(110)$) in the TPD experiments as shown in Fig. 2 (a) and (b). The similarity between the surface intermediates on $Mo_2C/Mo(110)$ and $Co/Mo_2C/Mo(110)$ are consistent with the similar HDO activities shown in the TPD results.

3.4. Reactor evaluation of powder catalysts: bridging the pressure and materials gaps

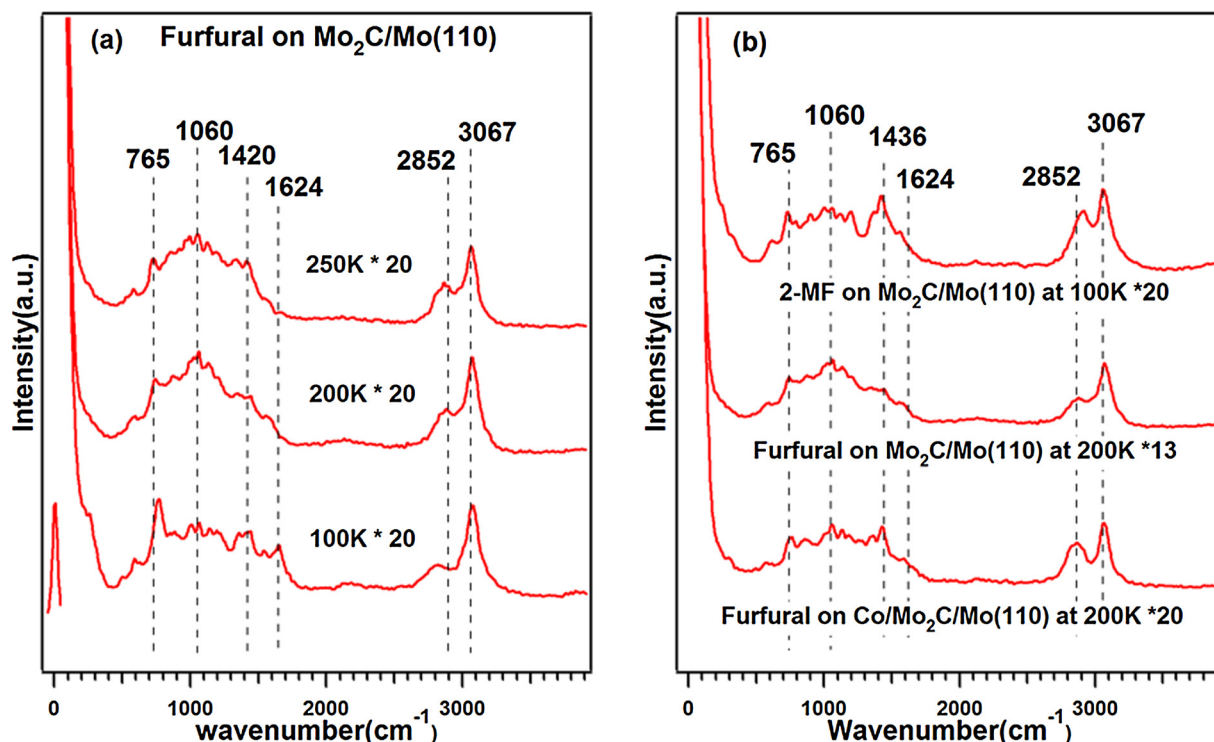Since DFT and TPD results suggested that $Co/Mo_2C/Mo(110)$ should

Fig. 3. HREEL spectra of (a) Furfural on $Mo_2C/Mo(110)$ at different temperatures and (b) 4 L 2-MF on $Mo_2C/Mo(110)$ at 100 K and 4 L furfural on hydrogen pre-dosed $Mo_2C/Mo(110)$ and $Co/Mo_2C/Mo(110)$ surfaces at 200 K.

be more stable than $Mo_2C/Mo(110)$ for the HDO reaction of furfural, porous Mo_2C and Co/Mo_2C catalysts were synthesized and a vapor phase flow reactor was used to evaluate the stability of the catalysts. XRD analysis on the spent Mo_2C and Co/Mo_2C catalysts was performed to verify the formation of Mo_2C. As shown in Fig. 4, the 2θ of 34.5°, 38.05°, 39.47°, 52.21°, 61.93°, 69.56°, 74.93° and 75.54° correspond to the (100), (002), (101), (102), (110), (103), (112) and (201) facets of β-Mo_2C (Joint Committee on Powder Diffraction Standards, no. 35-0787). With the addition of Co, the pattern does not change, likely due to the low loading of Co. In addition, since Mo_2C is a metal diffusion barrier, Co should remain on the surface of the Mo_2C particles.

The conversion of furfural (Fig. 5 (a)) and 2-MF yield (Fig. 5(b)) show the same trend, with the initial conversions (> 87%) and 2-MF yield (> 80%) being high on both Mo_2C and Co/Mo_2C with a subsequent decrease. The steady-state furfural conversion over Co/Mo_2C is approximately 35%, while that of Mo_2C drops to below 5%, confirming

that Co/Mo_2C is more stable than Mo_2C. The initial selectivity to 2-MF is above 90% for both Mo_2C and Co/Mo_2C. Over time, the selectivity to 2-MF decreases, although it remains as a major product over both catalysts. The selectivity to furan and furfuryl alcohol (FA) increases with reaction time over both catalysts, while the selectivity to tetrahydrofurfuryl alcohol (THFA) is always under 6%. It should be pointed out that FA and THFA were not detected in the TPD experiments on model surfaces, likely due to the different hydrogen partial pressure between the UHV and reactor environments. Overall, the flow reactor results are consistent with the trends from DFT calculations and UHV experiments on model surfaces, which show that $Co/Mo_2C/Mo(110)$ and $Mo_2C/Mo(110)$ have similar selectivity to 2-MF, but the stability of $Co/Mo_2C/Mo(110)$ is better than $Mo_2C/Mo(110)$, possibly due to the lower oxygen and furfural binding energies on $Co/Mo_2C/Mo(110)$. The general similarity between the behaviors of $Mo_2C/Mo(110)$ and $Co/Mo_2C/Mo(110)$ model surfaces and their corresponding powder catalysts suggests the feasibility of using surface science approaches to guide the design of efficient HDO catalysts.

4. Conclusions

Based on the results and discussion presented above, the following conclusions can be made regarding the potential utilization of Co/Mo_2C as an active and stable HDO catalyst:

(1) DFT calculations predict that the external carbonyl C=O bond in furfural is elongated on both $Mo_2C/Mo(110)$ and $Co-Mo_2C/Mo(110)$ surfaces due to the strong interaction between the carbonyl group and the surfaces, which should promote the C=O bond scission to form 2-MF. DFT calculations also indicate that the binding energies of oxygen and furfural on $Co/Mo_2C(0001)$ are weaker than on $Mo_2C(0001)$, suggesting that Co/Mo_2C might be more resistant to poisoning from surface oxygen, furfural and associated polymeric species.

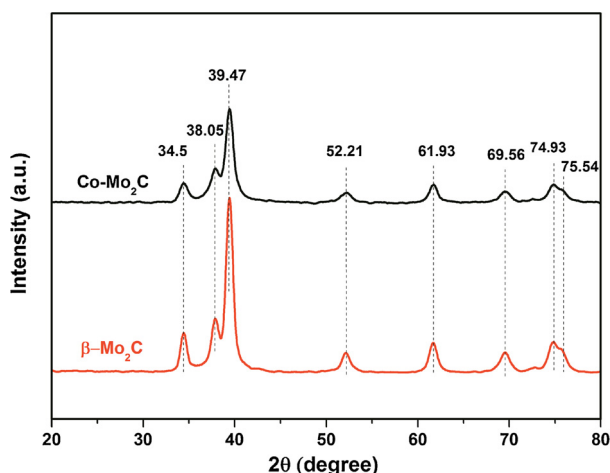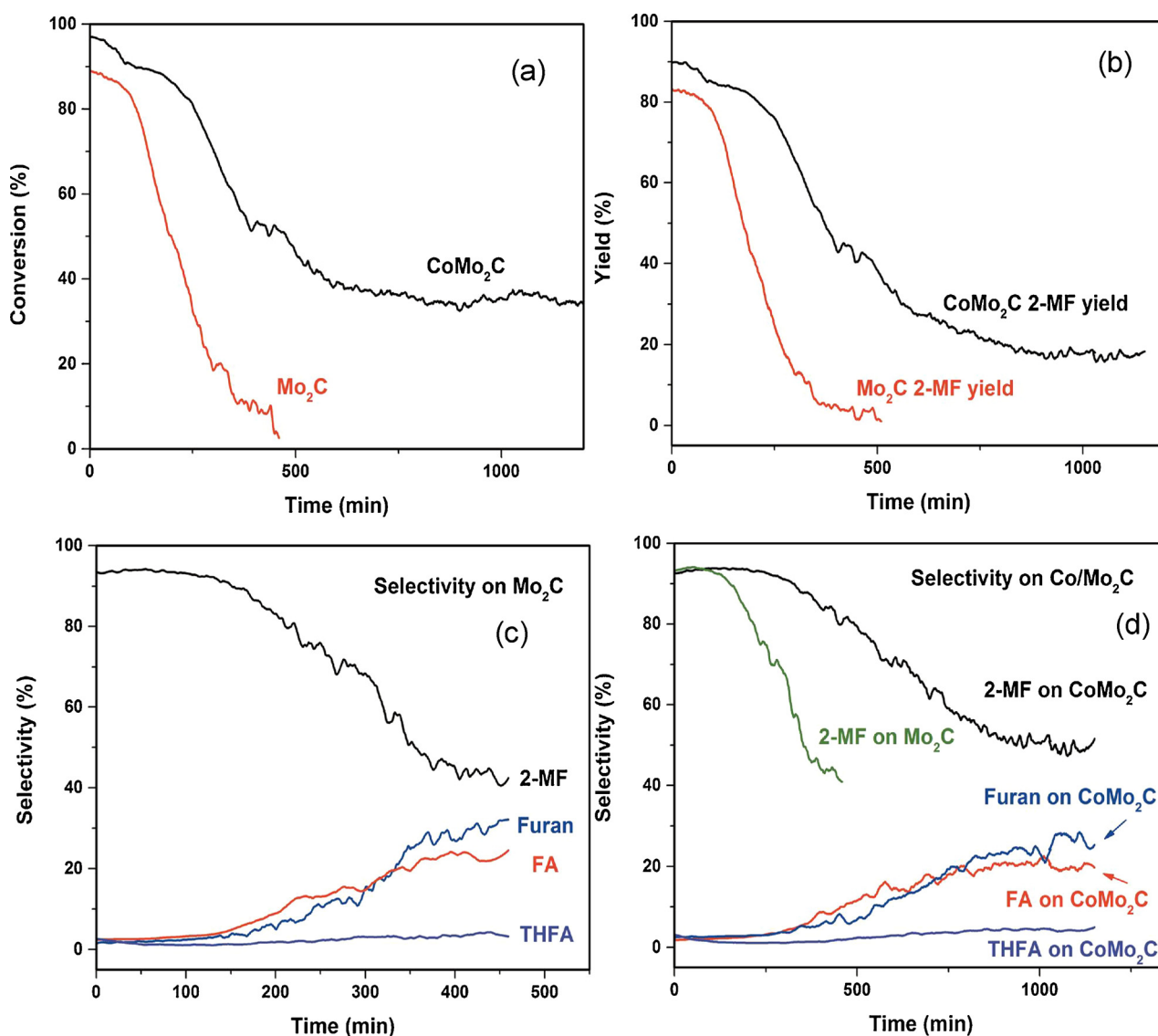(2) TPD results under UHV conditions verify the enhanced stability of

Fig. 4. XRD patterns of spent β-Mo_2C and 2 wt% Co/Mo_2C catalysts.

Fig. 5. Comparison of (a) furfural conversion, (b) 2-MF yield and (c), (d) products selectivity on Mo_2C and Co/Mo_2C. The selectivity to 2-MF on the Mo_2C catalyst (green) is shown in (d) for comparison. The furfural space velocity was 0.10 mL/(g_{cat}*s) as 20 mL/min of hydrogen flowed through a bubbler containing furfural preheated to 323 K. The molar ratio of hydrogen to furfural was 80 (For interpretation of the references to color in this figure legend, the reader is referred to the web version of this article).

$Co-Mo_2C/Mo(110)$ due to the facile removal of oxygen. HREELS results indicate that an intermediate similar to 2-MF is formed on $Mo_2C/Mo(110)$ and $Co-Mo_2C/Mo(110)$, consistent with the desorption of 2-MF in the TPD experiments.

(3) Parallel flow reactor evaluations on powder Mo_2C and $Co-Mo_2C$ catalysts further confirm the DFT predictions and surface science experiments that Co/Mo_2C is more stable than Mo_2C, while the HDO selectivity is similar for both catalysts.

(4) The general similarity between model surfaces and powder catalysts suggests the feasibility of using surface science approaches to identify promising catalyst candidates and using reactor studies to bridge the pressure and materials gaps.

Overall, it can be concluded that oxygen and furfural binding energies play an important role in stabilizing the catalyst for the furfural HDO reaction without affecting the HDO selectivity. This work shows the potential of modifying Mo_2C with metal overlayer to improve the catalyst stability and provides insights into the design of more efficient Mo_2C-based HDO catalysts for upgrading biomass-derived oxygenates.

Conflicts of interest

The authors declare no conflicts of interest.

Appendix A. Supplementary data

Supplementary material related to this article can be found, in the online version, at doi:https://doi.org/10.1016/j.apcatb.2018.03.113.

References

[1] J.N. Chheda, G.W. Huber, J.A. Dumesic, Liquid-phase catalytic processing of bio-mass-derived oxygenated hydrocarbons to fuels and chemicals, Angew. Chem. Int. Ed. 46 (2007) 7164–7183, http://dx.doi.org/10.1002/anie.200604274.

[2] G.W. Huber, A. Corma, Synergies between bio- and oil refineries for the production of fuels from biomass, Angew. Chem. Int. Ed. 46 (2007) 7184–7201, http://dx.doi.org/10.1002/anie.200604504.

[3] H. Wang, J. Male, Y. Wang, Recent advances in hydrotreating of pyrolysis bio-oil and its oxygen-containing model compounds, ACS Catal. 3 (2013) 1047–1070, http://dx.doi.org/10.1021/cs400069z.

[4] G.W. Huber, S. Iborra, A. Corma, Synthesis of transportation fuels from biomass: chemistry, catalysts, and engineering, Chem. Rev. 106 (2006) 4044–4098, http://dx.doi.org/10.1021/cr068360d.

[5] S.G. Wettstein, D. Martin Alonso, E.I. Gürbüz, J.A. Dumesic, A roadmap for con-version of lignocellulosic biomass to chemicals and fuels, Curr. Opin. Chem. Eng. 1 (2012) 218–224, http://dx.doi.org/10.1016/j.coche.2012.04.002.

[6] K. Xiong, W. Yu, D.G. Vlachos, J.G. Chen, Reaction pathways of biomass-derived oxygenates over metals and carbides: from model surfaces to supported catalysts, Chem. Cat. Chem. 7 (2015) 1402–1421, http://dx.doi.org/10.1002/cctc.201403067.

[7] J.P. Lange, E. Van Der Heide, J. Van Buijtenen, R. Price, Furfural-a promising platform for lignocellulosic biofuels, Chem. Sus. Chem. 5 (2012) 150–166, http://dx.doi.org/10.1002/cssc.201100648.

[8] L.W. Burnett, I.B. Johns, R.F. Holdren, R.M. Hixon, Production of 2-methylfuran by vapor-phase hydrogenation of furfural, Ind. Eng. Chem. 40 (1948) 502–505, http://dx.doi.org/10.1021/ie50459a034.

[9] S. Sitthisa, W. An, D.E. Resasco, Selective conversion of furfural to methylfuran over silica-supported NiFe bimetallic catalysts, J. Catal. 284 (2011) 90–101, http://dx.doi.org/10.1016/j.jcat.2011.09.005.

[10] W. Yu, K. Xiong, N. Ji, M.D. Porosoff, J.G. Chen, Theoretical and experimental studies of the adsorption geometry and reaction pathways of furfural over FeNi bimetallic model surfaces and supported catalysts, J. Catal. 317 (2014) 253–262, http://dx.doi.org/10.1016/j.jcat.2014.06.025.

[11] Z. Jiang, W. Wan, Z. Lin, J. Xie, J.G. Chen, Understanding the role of M/Pt(111) (M = Fe, Co, Ni, Cu) bimetallic surfaces for selective hydrodeoxygenation of furfural, ACS Catal. 7 (2017) 5758–5765, http://dx.doi.org/10.1021/acscatal.7b01682.

[12] J.G. Chen, C.A. Menning, M.B. Zellner, Monolayer bimetallic surfaces: experimental and theoretical studies of trends in electronic and chemical properties, Surf. Sci. Rep. 63 (2008) 201–254, http://dx.doi.org/10.1016/j.surfrep.2008.02.001.

[13] R.B. Levy, M. Boudart, Platinum-like behavior of tungsten carbide in surface cata-lysis, Science 181 (1973) 547–549, http://dx.doi.org/10.1126/science.181.4099.547.

[14] C.C. Tripathi, M. Kumar, D. Kumar, Atom beam sputtered Mo₂C films as a diffusion barrier for copper metallization, Appl. Surf. Sci. 255 (2009) 3518–3522, http://dx.doi.org/10.1016/j.apsusc.2008.09.076.

[15] H. Ren, W. Yu, M. Salciccioli, Y. Chen, Y. Huang, K. Xiong, D.G. Vlachos, J.G. Chen, Selective hydrodeoxygenation of biomass-derived oxygenates to unsaturated hy-drocarbons using molybdenum carbide catalysts, ChemSusChem 6 (2013) 798–801, http://dx.doi.org/10.1002/cssc.201200991.

[16] K. Xiong, W.S. Lee, A. Bhan, J.G. Chen, Molybdenum carbide as a highly selective deoxygenation catalyst for converting furfural to 2-methylfuran, ChemSusChem 7 (2014) 2146–2149, http://dx.doi.org/10.1002/cssc.201402033.

[17] P. Liu, J.A. Rodriguez, Water-gas-shift reaction on molybdenum carbide surfaces: essential role of the oxycarbide, J. Phys. Chem. B. 110 (2006) 19418–19425, http://dx.doi.org/10.1021/jp0621629.

[18] W. Yu, M. Salciccioli, K. Xiong, M.A. Barteau, D.G. Vlachos, J.G. Chen, Theoretical and experimental studies of C-C versus C-O bond scission of ethylene glycol reaction pathways via metal-modified molybdenum carbides, ACS Catal. 4 (2014) 1409–1418, http://dx.doi.org/10.1021/cs500124n.

[19] G. Kresse, J. Hafner, Ab initio molecular dynamics for liquid metals, Phys. Rev. B 47 (1993) 558–561, http://dx.doi.org/10.1103/PhysRevB.47.558.

[20] G. Kresse, J. Furthmüller, Efficiency of ab initio total energy calculations for metals and semiconductors using a plane wave basis set, Comput. Mater. Sci. 6 (1996) 15–50, http://dx.doi.org/10.1016/0927-0256(96)00008-0.

[21] G. Kresse, J. Furthmüller, Efficient iterative schemes for ab initio total-energy cal-culations using a plane-wave basis set, Phys. Rev. B 54 (1996) 11169–11186, http://dx.doi.org/10.1103/PhysRevB.54.11169.

[22] G. Kresse, D. Joubert, From ultrasoft pseudopotentials to the projector augmented-wave method, Phys. Rev. B 59 (1999) 1758–1775, http://dx.doi.org/10.1103/PhysRevB.59.1758.

[23] M.P. Teter, M.C. Payne, D.C. Allan, Solution of Schrodinger's equation for large systems, Phys. Rev. B 40 (1989) 12255–12263, http://dx.doi.org/10.1103/PhysRevB.40.12255.

[24] J. Perdew, J. Chevary, S. Vosko, K. Jackson, M. Pederson, D. Singh, C. Fiolhais, Atoms, molecules, solids, and surfaces: applications of the generalized gradient approximation for exchange and correlation, Phys. Rev. B 46 (1992) 6671–6687, http://dx.doi.org/10.1103/PhysRevB.46.6671.

[25] J.R. Kitchin, J.K. Nørskov, M.A. Barteau, J.G. Chen, Trends in the chemical prop-erties of early transition metal carbide surfaces: a density functional study, Catal. Today 105 (2005) 66–73, http://dx.doi.org/10.1016/j.cattod.2005.04.008.

[26] M. Salciccioli, W. Yu, M.A. Barteau, J.G. Chen, D.G. Vlachos, Differentiation of O-H and C-H bond scission mechanisms of ethylene glycol on Pt and Ni/Pt using theory and isotopic labeling experiments, J. Am. Chem. Soc. 133 (2011) 7996–8004, http://dx.doi.org/10.1021/ja201801t.

[27] J. Meng, C.A. Menning, M.B. Zellner, J.G. Chen, Effects of bimetallic modification on the decomposition of CH₃OH and H₂O on Pt/W(110) bimetallic surfaces, Surf. Sci. 604 (2010) 1845–1853, http://dx.doi.org/10.1016/j.susc.2010.07.015.

[28] H.H. Hwu, J.G. Chen, Reactions of methanol and water over carbide-modified Mo(1 1 0), Surf. Sci. 536 (2003) 75–87, http://dx.doi.org/10.1016/S0039-6028(03)00607-1.

[29] B. Frühberger, J.G. Chen, Reaction of ethylene with clean and carbide-modified Mo (110): converting surface reactivities of molybdenum to Pt-group metals, J. Am. Chem. Soc. 118 (1996) 11599–11609, http://dx.doi.org/10.1021/ja960656l.

[30] B. Frühberger, J.G. Chen, J.J. Eng, B.E. Bent, Reactivities of carbon- and ni-trogen-modified Mo(110) a comparison of modification effects by surface and in-terstitial adatoms, J. Vac. Sci. Technol. A Vac. Surf. Films 14 (1996) 1475–1481, http://dx.doi.org/10.1116/1.579972.

[31] M. Myint, Y. Yan, J.G. Chen, Reaction pathways of propanal and 1 propanol on Fe/Ni (111) and Cu / Ni (111) bimetallic surfaces, J. Phys. Chem. C 118 (2014) 11340–11349, http://dx.doi.org/10.1021/jp501208q.

[32] T. Kim, R.S. Assary, L.A. Curtiss, L. Marshall, P.C. Stair, Vibrational properties of levulinic acid and furan derivatives: Raman spectroscopy and theoretical calcula-tions, J. Raman Spectrosc. 42 (2011) 2069–2076, http://dx.doi.org/10.1002/jrs.2951.

[33] Y. Shi, Y. Yang, Y.W. Li, H. Jiao, Mechanisms of Mo₂C(101)-catalyzed furfural se-lective hydrodeoxygenation to 2-methylfuran from computation, ACS Catal. 6 (2016) 6790–6803, http://dx.doi.org/10.1021/acscatal.6b02000.